

Short Communication

Enhanced Biocompatibility and Corrosion Resistance of Plasma-Modified Biodegradable Magnesium Alloy

Sen Wu^{*}, Ya Zhang, Yu Shen, Xuehua Zhou, Qiurong Chen

Magnesium Alloy Technology Lab, Shanghai Institute of Microsystem and Information Technology, Chinese Academy of Science, Shanghai 200050, China.

*E-mail: u2_uestc@hotmail.com

Received: 17 June 2015 / *Accepted:* 15 July 2015 / *Published:* 26 August 2015

Because of the unique mechanical properties and biocompatibility, magnesium and its alloys have been intensively studied as biodegradable implant materials. But their poor corrosion resistance may result in the sudden failure of the implants. Plasma immersion ion implantation (PIII) is conducted to improve the poor corrosion properties of the Mg alloy in the simulated body fluid (SBF). Fluorine is implanted into the sample. The scanning electron microscopy and energy dispersive spectrometer are used to characterize the samples. The electrochemical corrosion behavior is investigated by potentiodynamic polarization. It is revealed that F-implanted Mg alloy have a lower corrosion rate. In addition, the immersion tests and the biocompatibility tests show that the F-implanted Mg alloy have the much better biocompatibility. It is indicated that the PIII with fluorine is a potential method to improve the biological properties of the Mg alloy.

Keywords: Magnesium alloy; PIII; degradation; biocompatibility

1. INTRODUCTION

Magnesium and its alloys are of growing interest for biomedical applications, as they have similar mechanic properties to natural bone [1-7]. These biomedical implants can degrade naturally and do not require a second surgery to remove them after tissues have healed sufficiently [8]. Compared to the traditional biomedical metal materials such as stainless steels and Ti, Mg alloy have some more excellent advantages: (1) magnesium and its alloy are the exceptionally lightweight metals with the specific gravity of approximate 1.7 g/cm³; (2) the elastic modulus of Mg alloys is closer to that of human bones; (3) magnesium can accelerate the growth of new bone tissue with harmless to human body; (4) Mg ion, the degradation products of Mg alloy, is essential to human metabolism.

However, magnesium has a high negative standard electrode potential and tends to corrode quickly in a human body environment.

Surface modification techniques, which are widely studied in recent years in order to reduce the corrosion rate of magnesium and its alloys, are believed to be necessary for Mg and its alloys as biomedical implants, and is also beneficial to improve the bioactivity [3,5,9-14]. Among these techniques, the plasma immersion ion implantation (PIII) is an excellent surface modification technique to improve the corrosion resistance of magnesium alloys by forming a stable passive layer on the surface. Several studies, associated with the ions implanted into magnesium and its alloys, have revealed that the implanted Mg alloy exhibited certain degrees of corrosion resistance enhancement [12-14]. Nevertheless, more ions implantation need to be developed to meet the stringent requirements of the implants. Fluoride, in the surface coating can improving the resistance of the Mg alloy, is one of the few know agents that can stimulate the osteoblast proliferation [15,16]. However, the effects of PIII with fluoride on the corrosion behavior of Mg alloy have been seldom explored.

In this work, we conducted the fluoride PIII into the magnesium. The features of morphology and composition were analyzed. To better understand the corrosion properties of bare and implanted Mg alloy, simulated body fluid (SBF) was used in the electrochemical tests and immersion tests. Moreover, hemolysis tests and cytotoxicity tests were also carried out to evaluate the biocompatibility of bare and F-implanted Mg alloy.

2. EXPERIMENTAL

The chemical compositions of the magnesium alloy employed in this study was as follows (in wt.%): Al 1.30%, Mn 0.2%, Zn 0.97%, Ni 0.001%, Cu 0.001%, La 0.08%, Pr 0.003%, Ce 0.2%, Fe 0.001%, and Mg balance. The samples were cut to the size of 15 mm×15 mm×5 mm. The magnesium alloy blocks were mechanically ground with #200, #400, #600, #800 emery paper sequentially. Before PIII, the samples were ultrasonically washed with distilled water sequentially and dried in air at room temperature. In this paper, all the solutions were prepared by using analytical grade reagents and distilled water.

The PIII was performed on the homemade ion implanter. A pulsed voltage of 20 kV with a pulse width of 200 μ s and pulsing frequency of 20 Hz was applied to the samples. The fluorine PIII was conducted by 300 W radio frequency (RF) and ion implantation lasted for 1 h.

The surface morphology of F-implanted Mg alloy (the fluorine PIII treated Mg alloy) was studied on a scanning electron microscopy (SEM, HITACHI, S-4700) equipped with an energy dispersive spectrometer.

The biodegradable properties were evaluated by electrochemical tests and immersion tests in the simulated body fluid (SBF). The concentrations (mmol/l) of the various ions in the SBF were: 142.0 Na⁺, 5.0 K⁺, 1.5 Mg²⁺, 2.5 Ca²⁺, 147.8 Cl⁻, 4.2 HCO₃⁻, 1.0 HPO₄²⁻, 0.5 SO₄²⁻. A 1 mol/l HCl solution was pipetted to adjust the pH to 7.5 at 37 °C.

The electrochemical corrosion behaviors of the implanted and bare magnesium alloy were studied on Autolab PGSTAT 302N electrochemical workstation. The samples exposure to the solution

was 0.5 cm^2 . Potentiodynamic polarization was conducted in a classical three electrodes cells at a constant voltage scan rate of $1 \text{ mV} \cdot \text{s}^{-1}$. The sample was the working electrode. A large area platinum sheet was used as counter electrode and a saturated calomel electrode (SCE) served as reference electrode.

The immersion test was carried out in the SBF. The immersion test was carried out at different time in order to monitor the corrosion rate of bare and PIII treated Mg alloy. The method for calculation of corrosion rate was presented in our previous work [11]. The temperature of the SBF maintains at $37 \pm 0.5^\circ\text{C}$. And the pH values of the SBF during immersion tests were monitored.

The hemolysis test and cytotoxicity test was carried out according to the national standard (China) of GB/T16886.4-2003 and GB/T16886.5-2003, respectively.

3. RESULTS AND DISCUSSION

3.1 Surface characteristics

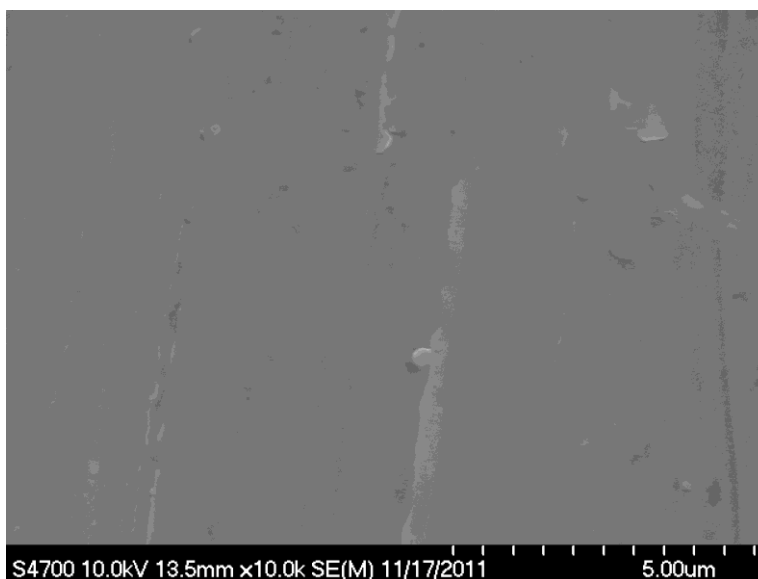


Figure 1. The surface morphology of the sample after fluorine PIII

Figure 1 displayed the morphology of the F-implanted Mg alloy. It was shown that the surface of the Mg alloy was relatively smooth regardless some cross striation which may be generated by the PIII treatment. This was indicated that the surface had almost no change after the PIII treatment.

It is well known that the PIII treatment can generate a stable passive layer on the surface to improve the corrosion resistance of Mg alloy. So, we have performed the EDS examination on the surface of PIII treated Mg alloy. It was clearly found that the passive layer mainly composed of O, F, Mg and Al as well as the trace of the Ti. It was indicated that the element of fluorine was successively implanted into to the surface of the Mg alloy. Hence, it was assumed that the passive layer may be mainly composed of MgO and MgF_2 , which may improve the corrosion resistance of the Mg alloy. It was noted that the element of Ti may come from the PIII equipment during the process.

Table 1. Element weight percent of F-implanted Mg alloy

	Weight (%)				
	O	F	Al	Mg	Ti
F-implanted sample	3.22	0.73	1.42	93.66	0.99

3.2 Electrochemical test

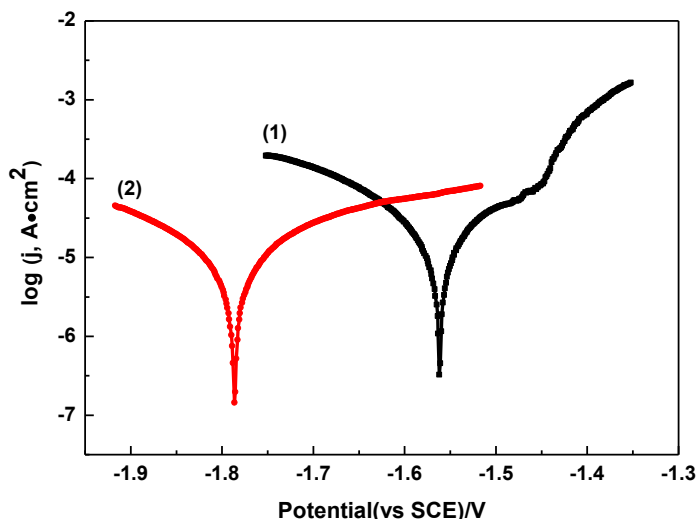


Figure 2. Potentiodynamic polarization behavior of (1) bare sample (2) F-implanted sample in the SBF

To examine the protection quality of the F-implanted Mg alloy, the potentiodynamic polarization measurement was carried out in the SBF solution, as shown in figure 2. The corrosion potential (E_{corr}), corrosion current density (j_{corr}) were obtained from potentiodynamic polarization curves in figure 2. These results are summarized in Table 2, based on the relationship [17]. It was obtained that the corrosion potential (E_{corr}) of the F-implanted sample shift toward the positive direction from -1.79 V to -1.56 V in the SBF. Moreover, there was a noticeable decrease in the corrosion current density (j_{corr}) from $8.59 \times 10^{-4} \text{ A/cm}^2$ to $2.97 \times 10^{-5} \text{ A/cm}^2$, which was about one order of magnitude smaller than that observed from the bare sample. In general, the results of potentiodynamic polarization according to figure 2 and Table 2 indicated the enhancement of corrosion resistance and the deceleration of degradation of Mg alloy after the PIII [18-20].

Table 2. Electrochemical parameters related to potentiodynamic polarization curves

	$E_{corr}(\text{V})$	$j_{corr}(\text{A/cm}^2)$
bare sample	-1.79	8.59×10^{-4}
F-implanted sample	-1.56	2.97×10^{-5}

3.3 Immersion test

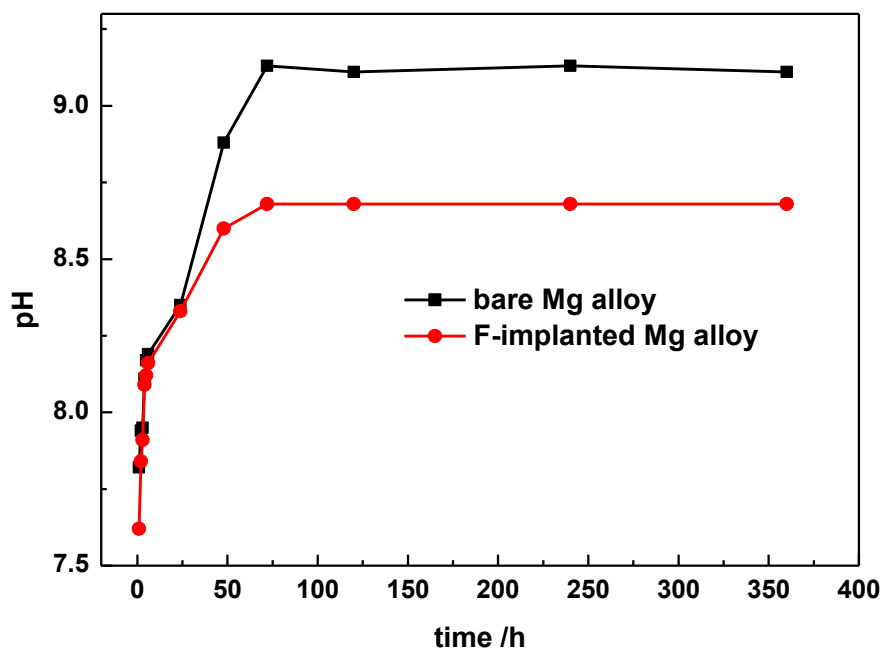


Figure 3. Change of pH values of bare and F-implanted Mg alloy in SBF

As the Mg alloy corroded in the SBF, the H^+ was consumed and the OH^- was released, which would result initially in an increase of local surface pH and subsequently an increase of pH in the bulk solution [21-26]. The magnesium could be corroded as follows:

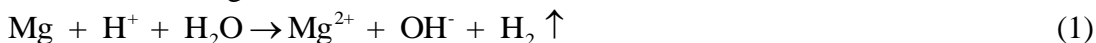


Figure 3 presented the changes of pH values of SBF immersing with the bare and F-implanted Mg alloy. It was interesting to note that the relative change in the pH values after different immersion time. During the initial 5 h, the pH values of bare and F-implanted Mg alloy were both increasing quickly with increasing immersion time, and the pH values of F-implanted Mg alloy was slightly lower than that of the bare Mg alloy. This was due to the release of the great number of OH^- in this stage. Between 5 and 72 h, although the pH values further increased, the growth trend has slowed down. It was noted that the pH value of bare Mg alloy was 9.2 with the immersion time of 72 h. Meanwhile, it was 8.7 for F-implanted Mg alloy lower than that of the bare Mg alloy. It was indicated that the surface of Mg alloy after the fluorine PIII treatment on could restrain the rate of alkalization. After 72 h, the pH values of bare and F-implanted both slightly decreased before stabilizing afterwards. This may due to the formation and dissolution of $Mg(OH)_2$ was arriving at the balance. The raise of the pH value promoted the formation of $Mg(OH)_2$. Meanwhile, the $Mg(OH)_2$ can restrain the rate of corrosion of the Mg alloy to some extent, the pH value decreased [27]. At the same time, the Cl^- in the SBF would react with $Mg(OH)_2$ to form the more soluble $MgCl_2$. In this frame, the pH value became stable.

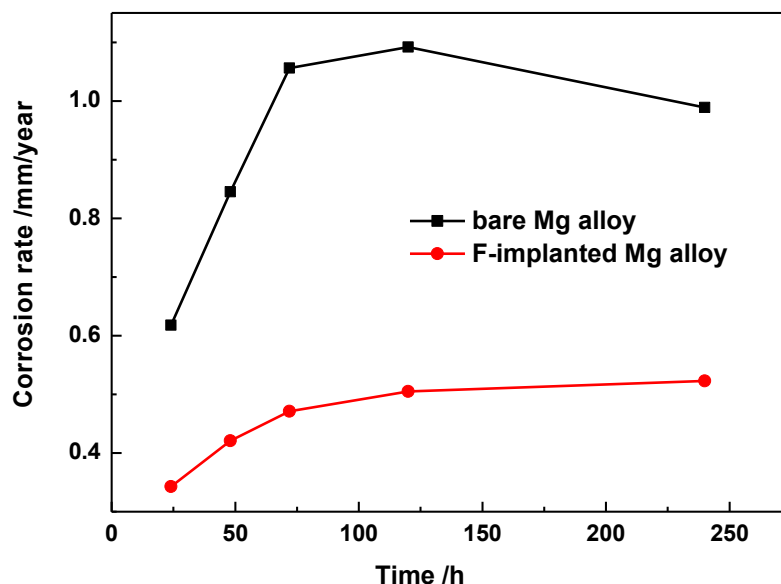


Figure 4. Corrosion rate of bare and F-implanted Mg alloy versus immersion time in the SBF

The corrosion rate of bare and Plasma-modified Mg alloy in the SBF was presented in figure 4. As seen from the Figure 4, the corrosion rate of bare Mg alloy increased from 0.6 mm/y to 1.05 mm/y, and almost stabilized at about 1 mm/y. However, the corrosion rate of bare Mg alloy increased from 0.34 mm/y to 0.5 mm/y. Hence, it was obtained that, the F-implanted Mg alloy either short or long-term provided excellent corrosion resistance compared to bare Mg alloy. The results of immersion tests are consistent with those of the electrochemical measurements, indicating effective protection proving by the F-implanted Mg alloy.

3.3 Biocompatibility test

The target of hemolysis test was the evaluation of the damage degree of the Mg alloy to red blood cells. And it must be carried out before the medical materials application in human body. Based on the immersion test, we found that the corrosion of Mg alloy in the SBF would release lots of OH⁻ ions, which affected the pH of the solution. As we know, these aspects would affect the blood red blood cells *in vivo*. The hemolysis tests of bare and F-implanted Mg alloys were shown in figure 5. It was presented that the hemolysis rate of bare Mg alloy was 55%, and 27% for the F-implanted Mg alloy, indicating the surface of Mg alloy after the PIII treatment having the protective effect towards to the red blood cells. Although the hemolysis rate has dropped obviously after PIII treatment, it has not reached the national standard (<5%). The amount of magnesium ions flowing into the blood made the pH of the blood rising rapidly, which led to the severe hemolytic phenomenon. The PIII treatment could prevent hemolytic phenomenon at a certain degree. However, due to the thin layer produced by the PIII treatment on the surface of the Mg alloy, the Mg ions were still capable of entering the blood

from the matrix. We will improve the experimental program to reduce the hemolysis rate of magnesium alloy in further.

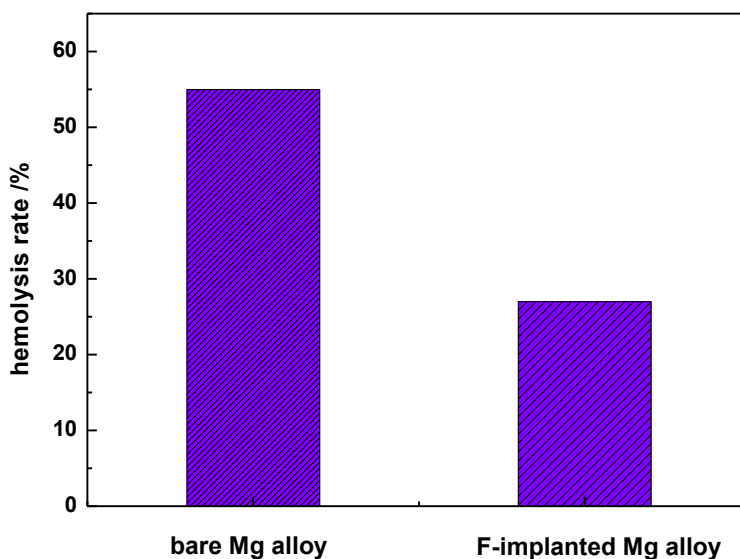


Figure 5. Hemolysis tests of bare and F-implanted Mg alloys

The results of cytotoxicity tests of bare and F-implanted Mg alloys were shown in Table 3. It was obtained that the Relative growth rate (RGR) of the bare Mg alloy exceeded 100%, arriving the ZERO grade of the national standard. Meanwhile, the RGR of the F-implanted sample Mg alloy which was 97.8%, arrived the one grade of the national standard. As we know, the results of the cytotoxicity tests were zero or one grade, the Mg alloy can be used as a biological implant material. This was indicated that the bare and F-implanted Mg alloy have no cytotoxicity and own excellent biocompatibility.

Table 3. Cytotoxicity tests of bare and F-implanted Mg alloys

	RGR	Grade
bare sample	>100%	0
F-implanted sample	97.8%	1

4. CONCLUSIONS

Magnesium alloy was treated by fluorine plasma immersion ion implantation. The process improved the corrosion resistance as inferred from the much more positive E_{corr} and much lower j_{corr} , compared to the bare Mg alloy in SBF. The immersion tests showed that the pH of the bulk solution and the corrosion rate of Mg alloy have been improved after fluorine PIII. The hemolysis and cytotoxicity tests presented that hemolysis rate was reduced after fluorine PIII, which have no

cytotoxicity. This was indicated that the fluorine PIII is a promising ways to improve the corrosion resistance and biocompatibility in the physiological environment.

ACKNOWLEDGEMENTS

This work was supported by Shanghai Scientific Research Projects (11DJ1400302).

References

1. F. Witte, V. Kaese, H. Haferkamp, E. Switze, *Biomaterials*, 26 (2005) 3557.
2. F. Witte, J. Fischer, J. Nellesen, H. Crostack, V. Kaese, A. Pischd, F. Beckmann, H. Windhagen, *Biomaterials*, 27 (2006) 1013.
3. X. Lin, X. Wang, L. Tan, P. Wan, X. Yu, Q. Li, K. Yang, *Ceram. Int.*, 40 (2014) 10043.
4. A. Alabbssi, S. Liyanaarachchi, M. B. Kannan, *Thin Solid Films*, 520 (2012) 6841.
5. M. Razavi, M. Fathi, O. Savabi, B. H. Beni, S. M. Razavi, D. Vasgae, L. Tayebi, *Appl. Surf. Sci.*, 288 (2014) 130.
6. N. T. Kirkland, N. Birbilis, M. P. Staiger, *Acta Biomater.*, 8 (2012) 925.
7. A. A. Ghoneim, A. M. Fekry, M. A. Ameer, *Electrochim. Acta*, 55 (2010) 6028.
8. M. P. Staiger, A. M. Pietak, J. Huadmai, G. Dias, *Biomaterials*, 27 (2006) 1728.
9. Y. W. Song, D. Y. Shan, E. H. Han, *Mater. Lett.*, 62 (2008) 3276.
10. L. Li, J. Gao, Y. Wang, *Surf. Coat. Technol.* 185 (2004) 92.
11. S. Wu, Y. Zhang, Z. Wei, Y. Shen, X. Zhou, Q. Chen, *Int. J. Electrochem. Sci.*, 9 (2014) 4394.
12. R. Xu, X. Yang, X. Zhang, M. Wang, P. Li, Y. Zhao, G. Wu, P. K. Chu, *Appl. Surf. Sci.*, 286 (2013) 257.
13. R. Xu, G. Wu, X. Yang, X. Zhang, Z. Wu, G. Sun, G. Li, P. K. Chu, *Appl. Surf. Sci.*, 258 (2012) 8273.
14. G. J. Wan, M. F. Maitz, H. Sun, P. P. Li, N. Huang, *Surf. Coat. Technol.* 201 (2007) 8267.
15. K. Y. Chiu, M. H. Wong, F. T. Cheng, H. C. Man, *Surf. Coat. Technol.* 202 (2007) 590.
16. T. Yan, L. Tan, D. Xiong, X. Liu, B. Zhang, K. Yang, *Mater. Sci. Eng. C*, 30 (2010) 740.
17. D. Y. Hwang, Y. M. Kim, D. -Y. Park, B. Yoo, D. H. Shin, *Electrochim. Acta*, 54 (2009) 5479.
18. X. Guo, M. An, P. Yang, H. Li, C. Su, *J. Alloys Compd.* 482 (2009) 487.
19. Y. Liu, Z. Wei, F. Yang, Z. Zhang, *J. Alloys Compd.* 509 (2011) 6440.
20. H.-Y Hsiao, H.-C. Tsung, W.-T Tsai, *Surf. Coat. Technol.* 199 (2005) 127.
21. C. Liu, Y. Xin, G. Tang, P. K. Chu, *Mater. Sci. Eng. A*, 456 (2007) 350.
22. M. Zhao, M. Liu, G. Song, A. Atrens, *Corros. Sci.*, 50 (2008) 3168.
23. Y. Wang, M. Wei, J. Gao, *Mater. Sci. Eng. C*, 29 (2009) 1311.
24. C. Lorenz, J. G. Brunner, P. Kollmannsberger, L. Jaafar, B. Fabry, S. Virtanen, *Acta Biomater.*, 5 (2009) 2783.
25. W. He, E. Zhang, K. Yang, *Mater. Sci. Eng. C*, 30 (2010) 167.
26. W. F. Ng, K. P. Chu, F. T. Cheng, *Mater. Sci. Eng. C*, 30 (2010) 898.
27. G. Song, *Adv. Eng. Mater.*, 7 (2005) 563

© 2015 The Authors. Published by ESG (www.electrochemsci.org). This article is an open access article distributed under the terms and conditions of the Creative Commons Attribution license (<http://creativecommons.org/licenses/by/4.0/>).